Volume 286, number 1,2, 193–200 FEBS 09898 July 1991

ADONIS 001457939100608S

Molecular basis for different rates of recovery from inactivation in the *Shaker* potassium channel family

Reilinde Wittka[2], Martin Stocker[1], Günther Boheim[2] and Olaf Pongs[1]

[1] *Ruhr-Universität Bochum, Lehrstuhl für Biochemie, Universitätsstr. 150, 4630 Bochum, Germany* and [2] *Ruhr-Universität Bochum, Lehrstuhl für Zellphysiologie, Universitätsstr. 150, 4630 Bochum, Germany*

Received 16 April 1991; revised version received 13 May 1991

The two alternative carboxyl-termini of *Shaker* K^+ channels strongly influence the rates of inactivation and of recovery from channel inactivation. We show that this distinct inactivation behaviour is due to an alanine/valine amino acid replacement within the *Shaker* carboxyl-terminus at a site that occurs within the proposed membrane spanning segment S6.

Potassium channel; *Shaker*; Macro-patch recording; *Xenopus* oocyte

1. INTRODUCTION

The *Shaker* (*Sh*) locus in the *Drosophila melanogaster* genome encodes a family of voltage-gated potassium channels [1–4]. Extensive cDNA analysis in several laboratories has identified so far 10 members of this potassium channel family [5–7]. The deduced protein sequences have five variant amino-termini, a common core region and two carboxyl-termini which are alternatively used. The expression of each protein in *Xenopus* oocytes induces the formation of functional K^+ channels [1–4,8,9]. Their characterization has indicated that they have variant electrophysiological properties. In particular, the kinetics of activation and inactivation as well as the recovery from inactivation are remarkably different among the various members of the *Sh* K^+ channel family. Recently, it has been shown that the amino-terminal sequences of *Sh* proteins have a profound influence on the kinetics of channel closure [4,9–11]. Both, natural variants and point mutations in the amino-terminus convert a rapidly inactivating into a slowly inactivating K^+ channel. These results suggested a model where the amino-terminus contains a cytoplasmic domain that interacts with the open channel to cause inactivation [10].

Also, the alternative carboxyl-termini play an important role in the kinetics of inactivation. Based on macroscopic current analysis, it has been suggested that the carboxyl-termini differently stabilize the inactivated states [9]. This might reflect the different rates at which the respective *Sh* K^+ channel recover from inactivation. We have carried out a mutational analysis in order to define the carboxyl-terminal domain involved which possibly serves as a receptor for the amino-terminal inactivation gate.

Correspondence address: O. Pongs, Ruhr-Universität Bochum, Lehrstuhl für Biochemie, Universitätsstr. 150, 4630 Bochum, Germany. Fax: (49) (234) 700 6837

Abbreviations: K^+, potassium; cRNA, cDNA derived mRNA; *Sh*, *Shaker*

2. MATERIALS AND METHODS

2.1. *In vitro mutagenesis and cRNA sythesis*

The point mutation *Sh*A2-A1463/464VV was introduced into pAS18-A2 [4] with the method of Herlitze et al. [12] using the mutation-primer A1463/464VV: TCACTTTGTGTCGTTGCTGGCGTG to mutate the *Nsi*I/*Hin*dII fragment (nt 1256–2151) of pAS18-A2, which then replaced the wild-type fragment in the starting clone.

Construction procedure for pAS18-A1 was the same as described for pAS18-A2 [4] except that the carboxyl-terminus of *Sh* class 1 members (cDNAβ in [6]) was used. *Sh*A1-V464I and *Sh*A1-VV463/464AI were generated as described in [13] using the mutation primers V464I:GTCGGCTCACTTTGTGTGATCGVTG-GTGTGCTG; VV463/464AI:TCTTTGTGCGCGATCGCTGGTG-TG. The mutated *Nsi*I/Asp718 fragments (nt 1292–1419) were cloned into *Nsi*I/Asp718 cut pAS18-A1 to replace the wild-type fragment. Mutant clones were controlled by sequencing.

The construction of the chimeric *Sh*A/RCK1 cDNA will be described elsewhere (Stocker et al., manuscript in preparation). pAS18-clones were linearized at the *Eco*RI site for cRNA synthesis according to a standard protocol [14].

2.2. *Electrophysiology*

Xenopus laevis oocytes were injected with cRNA and incubated for 2–3 days at 19°C [15]. All experiments were done at 20°C in normal frog Ringer solution of the following composition (in mM): NaCl 115, KCl 2.5, $CaCl_2$ 1.8, *Hepes* 10, pH 7.4. The kinetic properties of *Sh* channels were determined from macro-patch recordings in the cell attached configuration of the patch clamp technique [15] using an EPC7 (List). The oocyte inside potential was controlled by a separate electrode filled with 1 M KCl.

To determine the steady-state activation parameters, the function $G(V) = G_{max}/\{1 + \exp[(V_{\frac{1}{2}} - V)/a]\}$ was fitted to the conductance

values at each potential. The reversal potential was assumed to be -100 mV. Steady-state inactivation parameters were analyzed by fitting the function $G(V) = G_{max}/\{1 + \exp[(V - V_{1/2})/a]\}$ to the data points, using prepulses lasting 500 ms (test-pulse: +20 mV). Recovery from inactivation was measured using a conventional two-microelectrode voltage clamp. To estimate τ_R the function $I/I_{max} = C_0 - C_1 \times \exp(t/\tau_R)$ was fitted to peak maxima at various times. C_0 equals maximal recovery, $C_1 = 1/I_{max}$ at $t = 0$. All current data were filtered with 2 kHz (3 dB), low pass, and digitalized with 100 μs. Leak and capacitive currents had been subtracted using the P/4 method.

3. RESULTS

In this report we describe the properties of K^+ currents which are elicited in the *Xenopus* oocyte expression system by *Sh*A1 (*Sh*A in [5]) and *Sh*A2 (*Sh*B in [5] or *Sh*H4 in [7] protein, respectively. Both *Sh* proteins have the same amino-terminus 'A'. They differ in the carboxyl-terminal sequence, which corresponds either to the one of terminus 1 or terminus 2 as illustrated in Fig. 1A. The present topological model of K^+ channel subunits proposes that the protein contains six segments, S1–S6, which transverse the membrane. An additional hydrophobic region, H5, is probably the pore forming region tucked into the plane of the membrane between S5 and S6 [16–18]. The alternative carboxyl-termini start in front of the sixth putative transmembrane segment. The two alternative S6 segments differ in one amino acid at position 463 (valine vs alanine) (Fig. 1C). The alternative cytoplasmic sequences behind segment S6 differ at many places both, in sequence and in length (Fig. 1C).

The injection of *Sh*A1 cRNA into *Xenopus* oocytes leads to the expression of transient outward currents elicited by depolarizing steps to positive test potentials. Time course and voltage-dependence of activation were determined by measuring ensembele K^+ outward currents in cell-attached macro-patches (Fig. 2, Table I). In agreement with previous reports [1,2,8,9], which described whole-cell current recordings, these currents completely inactivate within 30 ms. The threshold of activation was at -40 to -50 mV. The current rises at 0 mV test potential from 10% to 90% of peak amplitude in 1.9 ± 0.5 ms ($n = 5$). The voltage of half-maximal activation $V_{n1/2}$ was -20.9 ± 14.7 mV ($n = 5$) and the voltage change for an *e*-fold increase in ensemble conductance a_n was 15 ± 1.5 mV ($n = 5$). The injection of *Sh*A2 cRNA into *Xenopus* oocytes leads to the expression of similarly transient outward currents (Fig. 2, Table I) in agreement with previously published data [1–4]. In contrast to *Sh*A1 currents, *Sh*A2 currents have a component representing 16.5 ± 7 ($n = 9$) of the transient peak current after a 200 ms pulse to +20 mV, which inactivates in the time range of seconds. Therefore, *Sh*A2 currents have a fast and a slow inactivation component (Table I).

The most significant difference between *Sh*A1 and *Sh*A2 currents is the different time course of recovery from inactivation. The time courses were determined in

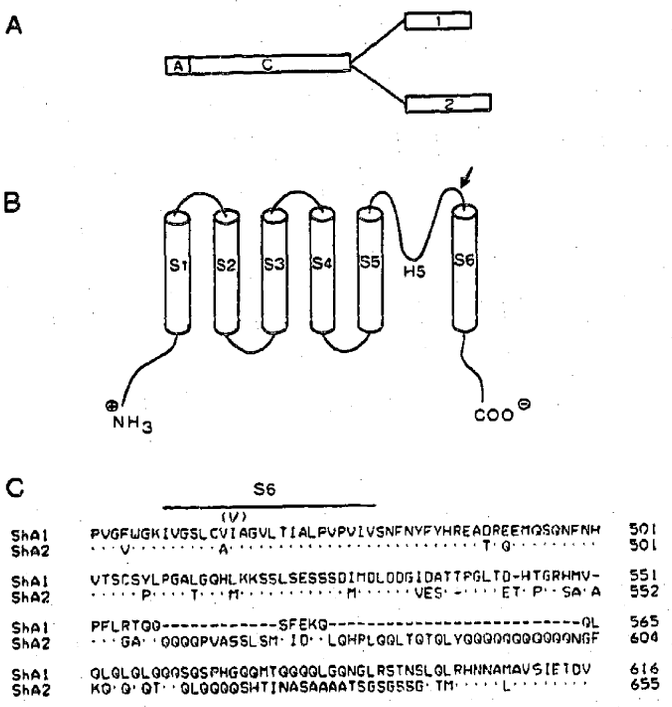

Fig. 1. General structure of *Sh*A1 and A2 K^+ channels. (A) Boxes illustrate the amino-terminal domain A connected to the core region C common to all *Sh* K^+ channel-forming proteins and the alternative carboxyl-termini 1 or 2. Box lengths are approximately to scale. Bar at lower right corresponds to 20 amino acids. Code for the nomenclature of other laboratories: *Sh*A1 = *Sh*A [1,5,8]; *Sh*A2 = *Sh*B [1,5,8] or *Sh*H4 [2,7,9]. (B) Topological model of *Sh* K^+ channel subunits inserted into the membrane having the N- and C-termini on the cytoplasmic side of the membrane. Segments S1 to S6 are possibly membrane spanning hydrophobic segments [6]. Segment H5 is probably tucked into the plane of the membrane being part of the conduction pathway [16–18]. Arrow indicates the splice site from which the alternative carboxyl-termini of *Sh*A1 and *Sh*A2 start. (C) Sequence alignment of the deduced *Sh* carboxyl-terminal protein sequences 1 and 2 [5–7]. Identical amino acids are indicated by dots. Dashes indicate gaps introduced for maximum sequence alignment. Numbers on the right and left hand side give the first and last amino acid residue number of the alternative carboxyl-terminal sequences. The sequence is given in a standard one letter code. Above residue 464 a valine in brackets marks a polymorphism between genomic DNA and cDNA-derived *Sh* sequences [5–7]. The hydrophobic segment S6 is delineated by a black bar.

two-pulse experiments (Fig. 2C,D). *Sh* currents were elicited by a pair of identical test pulses separated by a variable time, *t*. The first control test pulse to +20 mV elicits a large I_K appropriate for fully active *Sh* channels. The test pulse is long enough to activate and inactivate the *Sh* channels. Then the membrane is repolarized to -120 mV to initiate the removal of inactivation. Finally the second test pulse to +20 mV determines how far the recovery has proceeded after different times. As the interval between pulses is lengthened, the test I_K gradually recovers toward the control size (Fig. 2E,F). The recovery from inactivation is approximately described by an exponential function $[I/I_{max} = C_0 - C_1 \times \exp(t/\tau_R)]$, where τ_R is the time constant of recovery

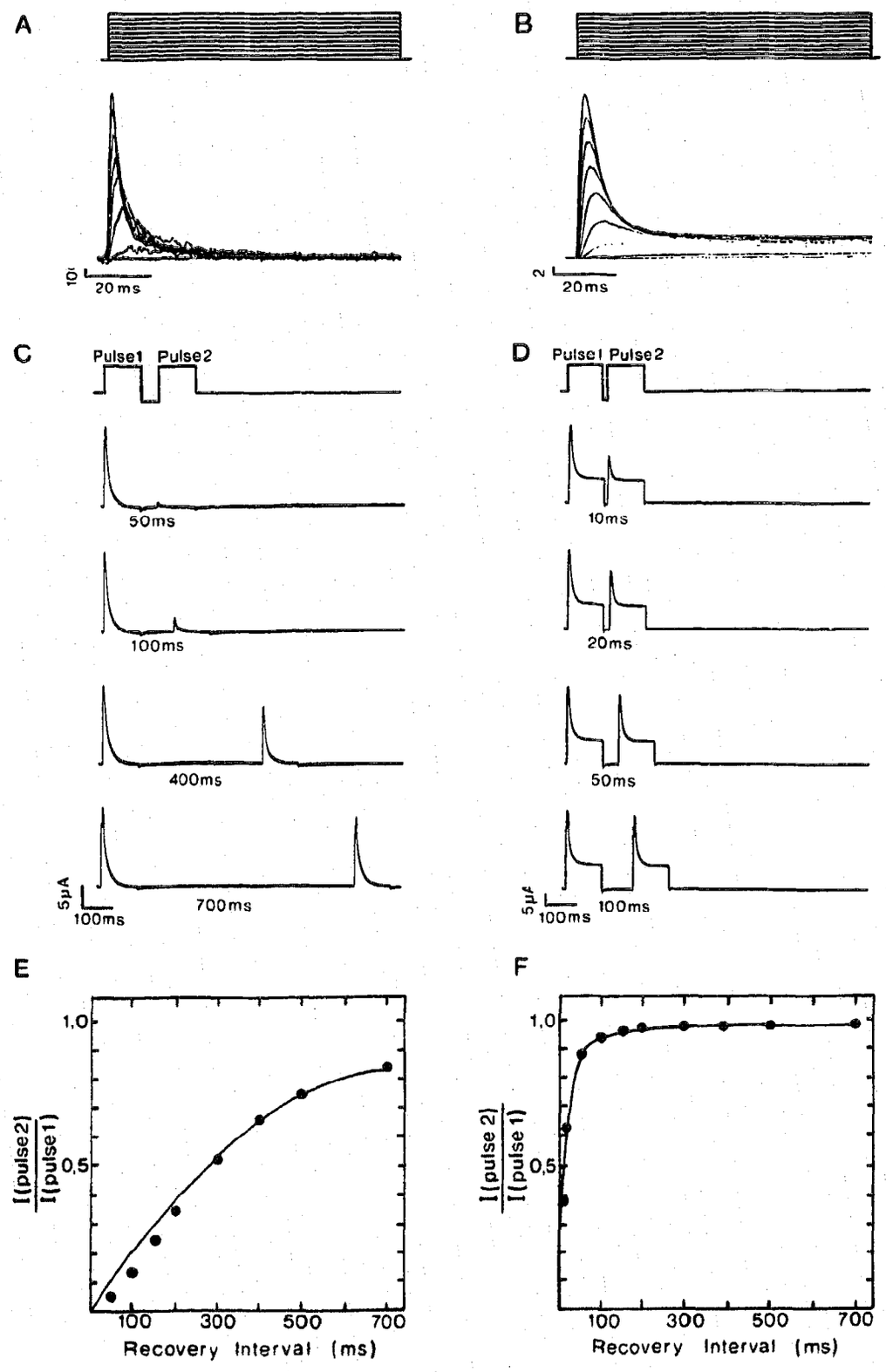

Fig. 2. Inactivation behaviour of *Sh*A1 and *Sh*A2 currents. Families of outward currents in response to depolarizing steps recorded from a macropatch in the cell-attached configuration. (A) *Sh*A1; (B) *Sh*A2. The traces are responses to 100-ms voltage steps from -80 to 20 mV in 10-mV increments from a holding potential of -80 mV as indicated by the pulse protocol on top. (C,D) Two-pulse experiments measuring the time course of recovery from *Sh*A1 (C) and *Sh*A2 (D) channel inactivation. A sample pulse protocol is given on top of the first current trace. Holding and interval potentials were at -80 and -120 mV. The first and second test pulse were to +20 mV. Interval times are indicated in milliseconds below each current trace. (E,F) Recovery curve shows the relation between recovery interval in ms versus the fraction of *Sh*A1 (E) or of *Sh*A2 (F) current which has recovered in that time.

Table I

		ShA2	ShA1	ShA2-AI463/4VV	ShA1-VV463/4AI
$V_{n1/2}$ (mV)[a]		-18.7 ± 13.8 (7)	-20.9 ± 14.7 (5)	-23.9 ± 14.7 (6)	-11.7 ± 8.5 (7)
a_n (mV)[b]		12.2 ± 2.5 (7)	15.0 ± 1.5 (5)	12.5 ± 4.0 (6)	14.5 ± 2.6 (7)
t_n (ms)[c]	0 mV	1.92 ± 0.37 (9)	1.88 ± 0.47 (5)	1.52 ± 0.28 (7)	2.32 ± 0.44 (9)
	20 mV	1.48 ± 0.27 (9)	1.36 ± 0.47 (5)	1.08 ± 0.22 (7)	1.73 ± 0.27 (9)
$V_{h1/2}$ (mV)[d]		-41.5 ± 13.8 (6)	-54.7 ± 20.8 (4)	-58.6 ± 14.8 (6)	-34.2 ± 10.2 (5)
a_h (mV)[e]		-4.7 ± 2.0 (6)	-9.0 ± 4.7 (4)	-5.9 ± 2.3 (6)	6.2 ± 1.6 (5)
$\frac{I_{3.2s}}{I_{peak}}$ (%)[f]	0 mV	6.0 ± 3.0 (3)			27.0 ± 12.0 (4)
	20 mV	5.2 ± 2.0 (3)			17.0 ± 7.0 (4)
$\frac{I_{0.2s}}{I_{peak}}$ (%)[g]	0 mV	22.9 ± 10.7 (9)			33.0 ± 9.0 (7)
	20 mV	16.5 ± 7.0 (9)			26.0 ± 8.0 (7)
τ_{i1} (ms)[h]	0 mV	8.4 ± 3.5 (7)	7.4 ± 6.1 (2)	5.5 ± 1.9 (8)	9.8 ± 2.1 (8)
	20 mV	6.4 ± 2.0 (7)	6.3 ± 3.4 (3)	4.3 ± 1.4 (8)	8.7 ± 2.3 (8)
τ_{i2} (s)[h]	0 mV	2.1 ± 0.9 (7)	0.10 ± 0.01 (2)	0.14 ± 0.11 (8)	2.51 ± 0.7 (8)
	20 mV	1.62 ± 0.2 (7)	0.08 ± 0.02 (3)	0.09 ± 0.04 (8)	1.59 ± 0.34 (8)

Numbers in parenthesis refer to number of experiments.

[a] Refers to test potential in mV where the conductance increase has reached one-half of its maximal value. The conductance was calculated for each potential by dividing the current amplitude by the driving force. The potassium reversal potential was calculated to be -100 mV. Ensemble current recording from macro-patches. Voltage steps were made from -80 mV holding potential.

[b] Refers to slope of normalized conductance-voltage relation. Its value corresponds to the change in test potential (in mV) to cause and *e*-fold increase in conductance.

[c] Refers to rise time of ensemble patch currents from 10% to 90% of the final current value. It was measured at 0 mV and 20 mV test potential following step changes from -80 mV holding potential.

[d] Refers to prepulse membrane potential in mV at which the current response to a step to 20 mV test potential is 50% of its maximal value. Prepulse duration is 500 ms. Holding potential was -80 mV. Ensemble currents from macro-patches.

[e] Refers to slope of steady-state inactivation curve. Change in prepulse membrane potential (in mV) to cause an *e*-fold reduction in the size of response to a test pulse to 20 mV.

[f,g] Refer to ratio of peak amplitude to amplitude at the end of a 3.2 s (f) or 200 ms (g) pulse at 0 and 20 mV test potential. Holding potential was -80 mV.

[h] Refers to decay time constants of inactivation at 0 and 20 mV test potential. Holding potential was -80 mV.

from inactivation. With interval pulses at -120 mV, the values of τ_R for *Sh*A1 and *Sh*A2 K^+ currents were ~400 ms and 20 ms, respectively. This result indicates that *Sh*A2 channels recover from inactivation ~20 times faster than *Sh*A1 channels.

The domains which determine the different rates of recovery from inactivation in *Sh*A1 and *Sh*A2 were defined by a mutational analysis. Firstly, we introduced behind segment S6 a bulk substitution of amino acid residues which are not identical between *Sh*A1 and *Sh*A2 in the carboxyl-terminus. This was accomplished by a replacement of the *Sh* carboxyl-terminus with the carboxyl-terminus of RCK1 [19], a K^+ channel, which very slowly inactivates in the min time range and immediately recovers from inactivation [20]. The resulting chimeric *Sh*A/RCK1 K^+ channel protein had an *Sh*A2 like segment S6, but behind segment S6 a carboxyl-terminal sequence which differed to *Sh*A2 at all the positions where the *Sh*A2 sequence is different from the *Sh*A1 sequence. The chimeric *Sh*A/RCK1 channels mediated transient outward currents which were very similar in their kinetic behaviour to *Sh*A2 channels. Also, a residual steady-state current representing ~15% of the transient peak current was observed (data not shown). A detailed description of the properties of this chimeric *Sh*A/RCK1 K^+ channel will be given elsewhere (M. Stocker et al., manuscript in preparation). The most likely interpretation of these results was that the carboxyl-terminal sequences behind segment S6 are not directly involved in K^+ channel activation and inactivation. Consequently, the differences in *Sh*A1 and *Sh*A2 segments S6 are probably responsible for the different inactivation behaviour of *Sh*A1 and *Sh*A2 K^+ channels. This hypothesis was tested by introducing reciprocal point mutations into *Sh*A1 and *Sh*A2. An *Sh*A1 channel protein with an *Sh*A2 like segment S6 having the sequence AI at positions 463 and 464, was generated by in vitro site directed mutagenesis of *Sh*A1 cDNA to *Sh*A1-VV463/4AI (see Methods). Conversely, an *Sh*A2 channel protein with an *Sh*A1 like segment S6 having the sequence VV at positions 463 and 464, was generated by in vitro site directed mutagenesis of *Sh*A2 cDNA to *Sh*A2-AI463/4VV.

Injection of *Sh*A1-VV463/4AI cRNA into *Xenopus* oocytes elicited the expression of transient outward currents with *Sh*A2 like properties (Table I). Most notably, the inactivation behaviour of *Sh*A1-VV463/4AI - channels was like that of *Sh*A2 channels (Table I, Fig. 3). Currents did not fall to baseline at the end of a 200 ms test pulse (Fig. 3A). The slowly inactivating compo-

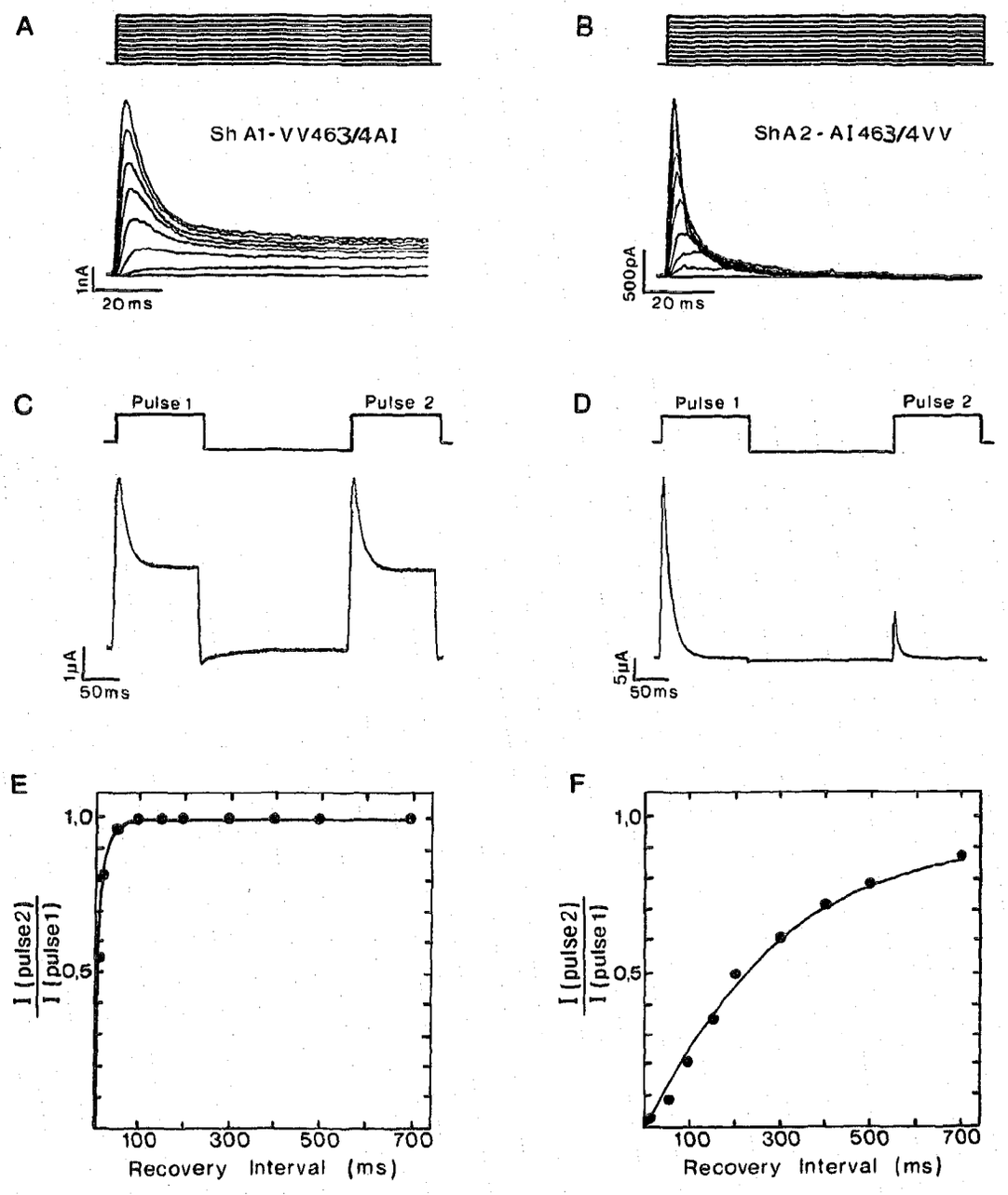

Fig. 3. Inactivation behaviour of *Sh*A1-VV463/4AI and of *Sh*A2-AI463/4VV currents. Families of outward currents in response to depolarizing steps recorded from a macro-patch in the cell-attached configuration. (A) *Sh*A1-VV463/4AI; (B) *Sh*A2-AI463/4VV. Experimental protocol as in Fig. 2. (C,D) Two-pulse experiment measuring the time course of recovery from *Sh*A1-VV463/4AI (C) and *Sh*A2-AI463/4VV (D) channel inactivation. The pulse protocol is as in Fig. 2. Interval times are indicated in ms below each current trace. (E,F) Recovery curve shows the relation between recovery interval in ms versus the fraction of *Sh*A1-VV463/4 (E) or of *Sh*A2-AI463/4VV current which has recovered in that time.

nent was 26 ± 8% ($n = 7$) of the transient peak current measured at 20 mV test potential. Also, the rate of recovery from inactivation as determined in two-pulse experiments (Fig. 3C) was like the one of *Sh*A2 currents. With interval pulses at -120 mV a value for τ_R of 12 ms was obtained for recovery from inactivation (Fig. 3E). This τ_R value is very similar to the 20 ms for recovery of *Sh*A2 currents (Fig. 2). Conversely, injection of *Sh*A2-AI463/4VV cRNA into *Xenopus* oocytes elicited the expression of transient outward currents which were similar to *Sh*A1 currents (Table I, Fig. 3). Now, the inactivation behaviour was like that of *Sh*A1 currents (Fig. 3B). The *Sh*A2-A/I463/4VV currents inactivated completely like *Sh*A1 currents and the rate of recovery from inactivation was as slow as that of *Sh*A1 currents (Fig. 3D,F). The value of τ_R which was determined in two-pulse experiments with interval pulses at -120 mV for removal of inactivation from

*Sh*A2-AI463/5VV channels, was 390 ± 235 ms. For comparison, the τ_R value for removal of inactivation from *Sh*A1 channels (Fig. 2E) was 360 ± 140 ms. These results indicate that the sequence difference between segment S6 of *Sh*A1 and *Sh*A2 is primarily responsible for the different inactivation behaviour of *Sh*A1 and *Sh*A2 K^+ channels. Since *Sh*A1-V464I cRNA expressed in oocytes *Sh*A1 like currents (data not shown), most likely the replacement of valine-463 to alanine suffices to impose *Sh*A1 like properties on *Sh*A2 and vice versa. It should be noted that the genomic sequence of *Sh* indicates only a difference in segment S6 sequences which corresponds to the valine-463/alanine exchange [6]. The additional occurrence of valine in derived carboxyl-terminus 1 sequences might be a cDNA cloning artefact or a *Drosophila* strain polymorphism. Also, sequencing of PCR products of *Sh*A1 and *Sh*A2 mRNA of a *Drosophila* Oregon R strain yields for both segments S6 at position 464 an isoleucine (data not shown).

The rate of recovery from inactivation of Na^+ channels is found to be voltage-dependent with a maximum at -60 mV near the normal membrane resting potential. T_R of recovery from inactivation of the *Sh* channels also depends on the recovery potential. The two-pulse experiments described in Figs. 2 and 3 were repeated with interval pulses at more positive potentials. At interval pulses more positive than -30 mV, it is difficult to separate rapid inactivation and recovery from inactivation in macroscopic current measurements. Therefore, recovery potentials in the two-pulse experiments ranged from -130 to -30 mV. A plot of τ_R against the recovery potential for *Sh*A2 and *Sh*A1-VV463/4AI channels shows similar bell-shaped curves (Fig. 4). The voltage-dependence of τ_R is not apparently affected. Maximum values of τ_R were measured at -40 mV recovery potentials near the threshold of *Sh* channel activation. The corresponding voltage-dependencies of τ_R for *Sh*A1 and *Sh*A2-AI463/4VV-channel inactivation were not determined. The times to recover toward the control size of *Sh*A1 and *Sh*A2-AI463/4VV-currents became so long (>10 s) with interval pulses above -100 mV that it was impractical to determine τ_R at more positive recovery potentials. At recovery potentials of -130 to -100 mV, however, τ_R is found to be voltage dependent similarly to T_R of *Sh*A2 and *Sh*A1-VV463/4AI, respectively (Fig. 4). Probably, this holds for the entire voltage dependence of τ_R. Combining the results shown in Figs. 2 to 4 indicates that alterations in the sequence of segment S6 have a profound influence on the rate of recovery of *Sh*A channels from inactivation.

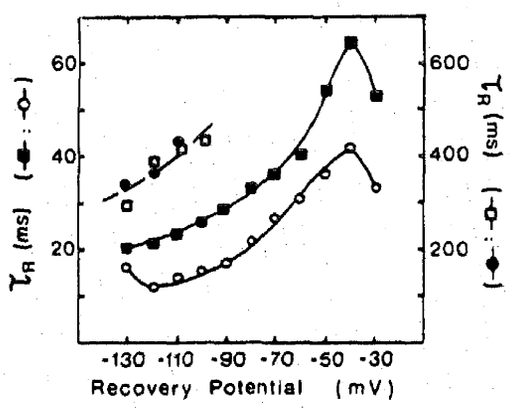

Fig. 4. Voltage-dependence of the time constant τ_R or recovery from inactivation measured as in Fig. 2 and 3. Pulse protocols were as in Fig. 2 and 3 except that the recovery potential was varied from -130 to -30 mV. Scale of τ_R on the left is for recovery of *Sh*A2 (●) and *Sh*A1-VV463/4AI (○) channels; scale of τ_R on the right is for recovery of *Sh*A1 (●) and *Sh*A2-AI463/4VV (□) currents.

4. DISCUSSION

The voltage-dependent gating of *Sh* channels is coupled to several molecular transitions associated with activation and inactivation. Some of the activation transitions leading to first opening of *Sh* channels are considerably voltage-dependent. In contrast, a kinetic analysis of data from single *Sh* channels in *Drosophila* muscle has suggested that all the molecular transitions after first opening, including the inactivation transition, are voltage independent [22]. All of the voltage dependence seen in the macroscopic currents can be accounted for by voltage-dependent activation transitions. A partially coupled model for activation and inactivation accurately reproduces the single-channel and macroscopic data of *Sh* channels [22,23]. Therefore, we did not consider alternative models, but have adopted the model in Scheme 1 to provide a framework in which to understand the different inactivation behaviour of *Sh*A1 and *Sh*A2 currents.

The rates α and β are dependent and the rates γ, δ, $\varkappa$, λ, ϵ and ν independent of voltage. Furthermore, we assume that the inactivated states I are not equivalent and that transitions are possible which allow the channel to recover from inactivation without opening. These transitions are determined by the rate constants ϵ and ν.

Members of the *Sh* channel family have distinct modes of inactivation [4, 8-10]. They inactivate rapidly in the millisecond time range and/or slowly in the second time range. Variations of the amino-terminus of *Sh* channels lead to altered rates of both, slow and fast inactivation [4, 8-10]. This is correlated with major alterations in the mean channel open times [4, 9, 10]. The most economical interpretation of these results can be obtained by assuming that the amino-terminus influences mainly the rate $\varkappa$ [4]. Alterations in the rate $\varkappa$ would alter the mean channel open time $1/(\delta+\varkappa)$ as well as the ratio between $\varkappa$ and λ which influences the stability of the non-absorbing inactivated state. Mutations in the *Sh*A2 amino-terminus that disrupt inactivation apparently decrease the rate $\varkappa$ and increase the rate λ [10]. The rates into (δ) and out of the closed state (γ) are not significantly altered. These data suggest a ball

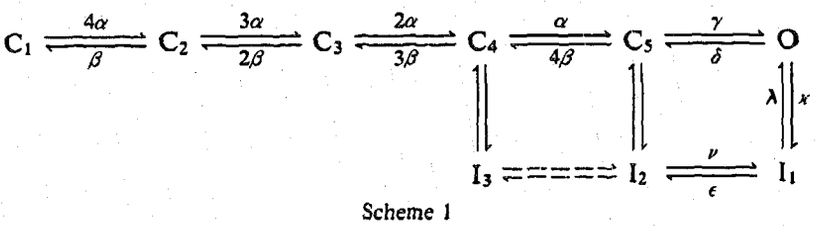

Scheme 1

and chain model where the amino-terminus contains a domain (ball) that interacts with the open channel to cause inactivation.

The distinct inactivation and recovery modes of *Sh* channels raise the possibility that the *Sh* channel has two types of inactivated states [9]. The direct transition of a closed to an inactivated state (C_4 to I_3 and/or C_5 to I_2 in Scheme 1) is not considered in this discussion. The first inactivated state (I_1) is non-absorbing. The second one (I_2) is basically absorbing and would be rate-limiting for the recovery from *Sh* channel inactivation. Our data indicate that the amino acid exchange between *Sh*A1 and *Sh*A2 segment S6 strongly influences the rate of recovery. This suggests that the stability of the absorbing inactivated state in *Sh* channels depends on the type of S6 sequence. From our model, the differences in kinetic behaviour of *Sh*A1 and *Sh*A2 channels can be accounted for by alterations in the rates which determine the transitions into the absorbing inactivated state (I_2). A simple assumption is that the nature of segment S6 influences mainly the time constant $1/(\lambda+\epsilon)$. In harmony with our data, an increase in the rate ϵ in *Sh*A1 type channels will then accelerate the transition from the first to the second inactivated state, slow-down the rate of recovery from inactivation, but will not influence the mean channel open time [9].

In the ball and chain model of inactivation, the 'inactivating ball' occludes the pore by interacting with a binding site(s) in the open channel. In the framework of our model, a weak interaction with a lifetime of a few milliseconds leads to a non-absorbing inactivated state (I_1). This might be followed by a stronger interaction with a 100 times longer lifetime which is correlated witht the transition into the second, absorbing inactivated state (I_2). This transition, which corresponds to the stability of the interaction of the 'inactivating ball' with the K^+ channel, is apparently strongly influenced by the nature of segment S6. Since the behaviour of *Sh*A1 and *Sh*A2 mutant channels was reciprocal, we believe that the exchange of alanine/valine-463 in *Sh*A channels does not introduce a global alteration of K^+ channel structure, but represents a local structural change within the binding site for the 'inactivating ball'. Alanine and valine are less or more hydrophobic amino acids. Consequently, the binding of the 'inactivating ball' to segment S6 should be at least in part a hydrophobic interaction. This notion is supported by two other experiments. The analogous exchange of alanine/valine in delayed rectifier type RCK1 channels [15] which do not possess an 'inactivating ball' does not alter their kinetic properties. Furthermore, a mutational analysis of the 'inactivation ball' [10] suggested that it requires a hydrophobic domain for its activity. Finally, our data indicate that τ_R is voltage-sensitive over the range of recovery potentials tested. Different factors may contribute to this voltage-dependence. According to Scheme 1, activation and inactivation are not independent from each other. Therefore, any voltage-sensitive transition, e.g. channel activation, will contribute to an apparent voltage-dependence of recovery from inactivation. In addition, occulusion of the channel pore by the 'inactivation ball' probably takes place near and/or within the electric field of the membrane. Accordingly, the positively charged domain of the 'inactivation ball' [10] may evoke a voltage-dependence of recovery from inactivation. Yet another alternative is a voltage-dependent transition of *Sh* K^+ channels necessary to release the 'inactivation ball' from its binding site.

Acknowledgements: We thank Dr. J.P. Ruppersberg for helpful discussions. This work was supported by grants of Deutsche Forschungsgemeinschaft.

REFERENCES

[1] Tempel, B.L., Jan, Y.N. and Jan, L.Y. (1988) Nature 332, 837–839.
[2] Iverson, L.E., Tanouye, M.A., Lester, H.A., Davidson, N. and Rudy, B. (1988) Proc. Natl. Acad. Sci. USA 85, 5723–5727.
[3] Zagotta, W.N., Hoshi, T. and Aldrich, R.W. (1989) Proc. Natl. Acad. Sci. USA 86, 7243–7247.
[4] Stocker, M., Stühmer, W., Wittka, R., Wang, X., Müller, R., Ferrus, A. and Pongs, O. (1990) Proc. Natl. Acad. Sci. USA 87, 8903–8907.
[5] Schwarz, T.L., Tempel, B.L., Papazian, D.M., Jan, Y.N. and Jan, L.Y. (1988) Nature 331, 137–142.
[6] Pongs, O., Kecskemethy, N., Müller, R., Krah-Jentgens, I., Baumann, A., Kiltz, H.H., Canal, I., Llamazares, S. and Ferrus, A. (1988) EMBO J. 7, 1087–1096.
[7] Kamb, A., Tseng-Crank, J. and Tanouye, M. (1988) Neuron 1, 421–430.
[8] Timpe, L.C., Jan, Y.N. and Jan, L.Y. (1988) Neuron 1, 659–667.
[9] Iverson, L.E. and Rudy, B. (1990) J. Neurosci. 10, 2903–2916.
[10] Hoshi, T., Zagotta, W.N. and Aldrich, R.W. (1990) Science 250, 533–538.
[11] Zagotta, W.N., Hoshi, T. and Aldrich, R.W. (1990) Science 250, 568–570.
[12] Herlitze, S. and Koenen, M. (1990) Gene 91, 143–147.

[13] Nelson, R.M. and Long, G.L. (1989) Anal. Biochem. 180, 147–151.
[14] Krieg, C. and Melton, D.A. (1984) Nucleic Acids. Res. 12, 7057–7070.
[15] Stühmer, W., Ruppersberg, J.P., Schröter, K.H., Sakmann, B., Stocker, M., Giese, K.P., Perschke, A., Baumann, A. and Pongs, O. (1989) EMBO J. 8, 3235–3244.
[16] Yool, A.J. and Schwarz, T.L. (1991) Nature 349, 700–704.
[17] Yellen, G., Jurman, M.E., Abramson, T. and MacKinnon, R. (1991) Science 251, 939–942.
[18] Hartmann, H.A., Kirsch, G.E., Drewe, J.A., Taglialatela, M., Joho, R.H. and Brown, A.M. (1991) Science 251, 942–944.
[19] Baumann, A., Grupe, A., Ackermann, A. and Pongs, O. (1988) EMBO J. 7, 2457–2463.
[20] Stühmer, W., Stocker, M., Sakmann, B., Seeburg, P., Baumann, A., Grupe, A. and Pongs, O. (1988) FEBS Lett. 242, 199–206.
[21] Hille, B. (1984) Ionic Channels of Excitable Membranes, Sinauer Assoc., Sunderland, MA.
[22] Zagotta, W.N. and Aldrich, R.W. (1990) J. Gen. Physiol. 95, 29–60.
[23] Zagotta, W.N. and Aldrich, R.W. (1990) J. Neurosci. 10, 1799–1810.